doi:10.1016/j.jmb.2007.10.022 J. Mol. Biol. (2007) 374, 910–916

JMB

Available online at www.sciencedirect.com

ScienceDirect

ELSEVIER

COMMUNICATION

Ultrastructural Analysis of the Nuclear Localization Sequences on Influenza A Ribonucleoprotein Complexes

Winco W. H. Wu, Lindsay L. Weaver and Nelly Panté*

Department of Zoology, University of British Columbia, 6270 University Boulevard, Vancouver, BC, Canada V6T 1Z4

Received 26 July 2007; received in revised form 28 September 2007; accepted 10 October 2007
Available online 13 October 2007

The influenza A genome consists of eight single-stranded RNA molecules, each associated with an oligomeric core of the structural protein, nucleoprotein, to form a distinct viral ribonucleoprotein (vRNP) complex. vRNPs are the entities responsible for the transcription and replication of the influenza viral RNAs in the nuclei of host cells. Thus, nuclear targeting and localization of the vRNPs are a critical step in the infection and life cycle of influenza A. We have recently shown that the nuclear import of vRNPs derived from influenza A virions is independently mediated by two nuclear localization sequences (NLSs) on nucleoprotein: NLS1, spanning residues 1–13 at the N terminus, and NLS2, spanning residues 198–216 in the middle of the protein, with NLS1 being the principal mediator. To better understand the structural basis for the differences in the ability of NLS1 and that of NLS2 to mediate nuclear import of influenza vRNPs, we analyzed the levels of surface exposure of these NLSs on vRNPs by both dot blotting and immunogold labeling of vRNPs in their native state. We found that NLS1 is much more accessible to its corresponding antibody compared with NLS2. Electron microscopy of immunogold-labeled vRNPs further showed that 71% of vRNPs were labeled with one to six gold particles located throughout the vRNP for NLS1. In contrast, less than 10% of vRNPs were labeled with an antibody against NLS2, usually with a single gold particle located at one end of the vRNP. In addition, a regular periodicity of repeat was observed with gold particles labeling for NLS1, indicative of a highly regular helical conformation present in the vRNPs. These findings provide the underlying structural basis for the enhanced ability of NLS1 in mediating nuclear import of influenza vRNPs and add to our understanding of the ultrastructural features of vRNP complexes derived from influenza A virions.

Keywords: immunogold; influenza virus; nuclear localization sequence; ribonucleoprotein complex; RNP

Edited by W. Baumeister

The influenza A viral genome consists of eight single-stranded, negative-sense viral RNA (vRNA) molecules of varying lengths. Each strand of the RNA genome is individually stabilized by multiple copies of nucleoprotein (NP; ~56 kDa) and assembled into viral ribonucleoprotein (vRNP) complexes, with each vRNP also containing a single copy of a trimeric vRNA polymerase complex (reviewed in Ref. 1). Within the influenza virus, these vRNPs are enclosed by a viral envelope and are organized into a distinct pattern with seven vRNPs in a circle surrounding one vRNP at the center,[2,3] although such a regular pattern may often

**Corresponding author.* E-mail address: pante@zoology.ubc.ca.

Abbreviations used: vRNP, viral ribonucleoprotein; vRNA, viral RNA; NLS, nuclear localization sequence; NP, nucleoprotein; TEM, transmission electron microscopy; PBS, phosphate-buffered saline; TBST, Tris-buffered saline Tween-20; BSA, bovine serum albumin.

not exist. The size and shape of the influenza virions even for a single strain are variable, with smaller-sized virions having fewer than eight vRNP molecules.[3]

The structure of influenza vRNPs has been studied in some detail using electron microscopy. Influenza vRNPs consist of long helical rods of variable size ranging from approximately 30 to 110 nm.[4] It is well established that oligomeric NP forms the helical core of the vRNP around which the vRNA is wrapped.[5] Approximately 24 nt associate with each NP.[4,6] Thus, given that each vRNA is about 890–2341 nt long (reviewed in Ref. 1), each influenza vRNP has 37–97 copies of NP. The structure of the influenza vRNP results from the ability of NP to oligomerize and to bind to RNA. Even during the course of influenza infection, dimers and trimers of NP have been detected, indicating that those are likely the smallest units from which vRNPs first assemble.[7] Analysis of NP deletion mutants has identified two regions of NP that are important for self-association: one at the middle of the molecule and the second at the C-terminal third of NP.[8] More recently, the crystal structure of the NP trimer has been solved and reveals that the NP molecule has a crescent shape with a tail loop.[9] The tail loop consists of amino acid residues 402–428 on NP and mediates NP oligomerization in such a way that the tail loop of one NP molecule inserts into the body segment of an adjacent NP molecule.[9] In addition to identifying the oligomerization site, the crystal structure of trimeric NP also reveals a possible RNA-binding groove made up of a large number of surface-exposed basic residues.[9] Analysis of the crystal structures of the NP from three negative-strand RNA virus families has also suggested that the RNA-binding cavity on influenza NP may be formed by two domains composed of amino acid residues 58–148 and 222–271.[10]

Influenza vRNPs are the entities responsible for the transcription and replication of the viral genome. These critical cellular processes in the life cycle of influenza A occur in the nuclei of host cells. Thus, influenza vRNPs must enter the nucleus of their host cells in order to establish a productive infection. The nuclear transport of vRNPs occurs after the influenza virion containing these incoming vRNPs is internalized into an endosome. The vRNPs are then released into the cytoplasm by fusion of the viral and endosomal membranes, which is triggered by the acidic environment of the endosome. Once in the cytoplasm, the vRNPs must use an exposed nuclear localization sequence (NLS) to help mediate their nuclear import. NP contains at least two NLSs: NLS1 (also termed the nonclassical or unconventional NLS, spanning residues 1–13 at the N terminus) and NLS2 (also termed the classical bipartite NLS, spanning residues 198–216 in the middle of the protein) (Fig. 1a).[12–15] Demonstration that both NLS1 and NLS2 can function as NLSs has been shown through the fusion of these NLSs to cytoplasmic reporter proteins, which then localize to the nucleus.[14,15] In contrast to these chimeric proteins, however, the NLSs on intact vRNPs may be masked by the interaction of NP with other NP molecules or with the vRNA.

The contribution of NLS1 and NLS2 to the nuclear import of the influenza genome has recently begun to become elucidated.[12,16,17] Studying nuclear import of *in vitro* assembled NP–vRNA complexes in the absence or presence of competitive peptides carrying NLS1, Cros *et al.*[16] found that the NLS1 peptide efficiently inhibited the nuclear import of these complexes. However, using vRNPs isolated from influenza A virions, we found that both NLS1 and NLS2 contribute to the nuclear import of vRNPs.[12] NLS1 and NLS2 act independently of each other, as inhibition of only one of the two NLSs still resulted in significant, though diminished, nuclear import of vRNPs. Similarly, Ozawa *et al.*[17] found that mutation of either NLS1 or NLS2 eliminated some nuclear import of influenza vRNPs but did not abolish it completely. In all these studies, however, the nuclear localization signal from NLS1 appeared to be a more potent mediator of nuclear import than that from NLS2.[14,12,17]

To better understand the structural basis for the different roles of NLS1 and NLS2 in the nuclear import of influenza vRNP, we further analyzed the NLSs on vRNP complexes obtained from purified influenza A virions. As revealed by negative staining and visualization by transmission electron microscopy (TEM), these purified vRNPs had the expected structure of an elongated helical rod with variable length of 30–120 nm (Fig. 1b). To evaluate the exposure of NLS1 and NLS2 on the outer surface of the purified vRNPs, we performed dot-blot immunostaining assays using anti-NLS1 and anti-NLS2 antibodies. As illustrated in Fig. 1c, both antibodies revealed strong immunoreactive spots when their cognate peptides were subjected to dot-blot immunoassays, even at a fivefold dilution of the peptide. Judging by the darkness of the dots, we inferred that both antibodies bound equally well to their specific peptides. However, when purified vRNPs were subjected to the dot-blot immunoassay, the anti-NLS1 antibody showed a much more intense dot than the anti-NLS2 antibody (Fig. 1c). This decreased intensity for the anti-NLS2 antibody in binding to the vRNPs might be due to the blockage of NLS2 with the vRNA. To test this hypothesis, we incubated the vRNPs with a high concentration of salt (1.6 M NaCl) before the dot-blotting assay. This treatment should be able to disrupt critical ionic contacts between the negatively charged vRNA molecules and the surface-exposed, positively charged basic residues on NP. As illustrated in Fig. 1c, this treatment increased the intensity of the immunoreactive dots compared with untreated samples. It therefore appears that both NLS1 and NLS2 become more exposed and can be more readily recognized by the antibodies at a high salt concentration. However, the NLS1 immunoreactive spot was still more intense than the NLS2 spot. This may be explained if NP is still in

oligomeric form at a high salt concentration and the NLS2 is engaged in NP–NP interactions. Indeed, this seems to be the case because negative staining electron microscopy revealed that the vRNPs subjected to a high salt concentration looked similar to those that were untreated (data not shown). As a negative control, dot blotting in the absence of the primary antibodies was performed for each blot, and no signal was observed for any of those blots (Fig. 1c).

Two possible explanations can be inferred from the results of the immuno-dot-blot assays: (1) NLS1 is more densely exposed on the vRNPs than NLS2 or (2) NLS1 is exposed on a greater number of vRNP molecules than NLS2. To decide between these two possibilities, we performed immunoelectron microscopy of the purified vRNPs using the antibodies against NLS1 or NLS2 and secondary antibodies conjugated to 10-nm gold particles. As shown in Fig. 2a, this immunogold labeling was highly specific for the vRNP molecules, as shown by the low amount of free gold present. Furthermore, Fig. 2a demonstrates that the anti-NLS1 antibody bound to more molecules of vRNPs and bound more to

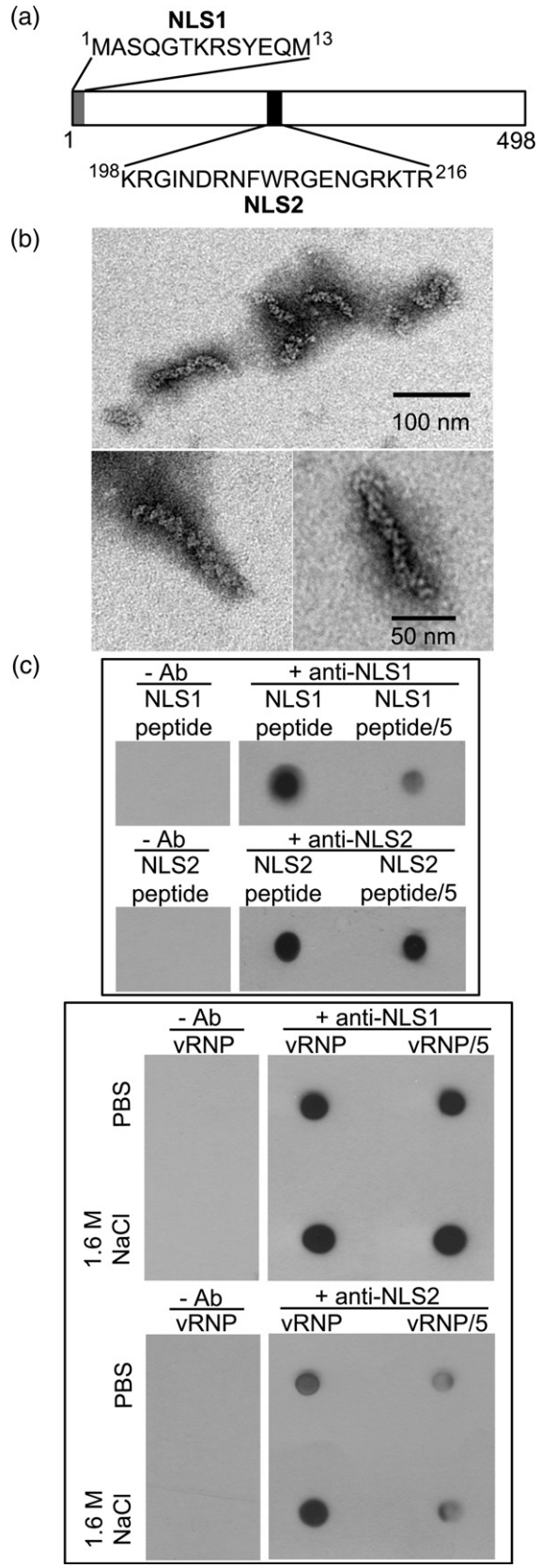

Fig. 1. (a) Schematic diagram of influenza A NP and the locations of the NLSs on the protein. (b) Electron microscopy visualization of influenza A vRNPs. Influenza A vRNPs were purified by glycerol gradient centrifugation according to the method of Kemler *et al.*[11] with modifications as previously described.[12] Electron microscopy grids (200 mesh; Ted Pella, Redding, CA) were freshly coated with 2% parlodion and carbon. Purified vRNPs (6 μl) in phosphate-buffered saline (PBS) were placed on these grids and allowed to be absorbed for 8 min. The solution was then removed; the grid was washed with PBS and negatively stained with 1% ammonium molybdate for 1 min. Samples were visualized under a Hitachi H7600 TEM (Hitachi High Technologies America, Schaumburg, IL). (c) Dot-blotting immunoassay with anti-NLS1 or anti-NLS2 antibodies. Peptides containing the sequence of either NLS1 (^{1}MASQGTKRSYEQM^{13}) or NLS2 (^{198}KRGINDRNFWRGENGRKTR^{216}) of influenza A NP were synthesized by Pacific Immunology (San Diego, CA). Polyclonal antibodies to each of these peptides were also produced and affinity purified by Pacific Immunology. Four microliters of the NLS1 peptide or the NLS2 peptide (at a concentration of 1.3 mM in PBS), or of purified vRNPs, was applied onto nitrocellulose membranes and allowed to dry. In some samples, the vRNPs were first denatured by incubating in a final salt concentration of 1.6 M NaCl for 10 min at room temperature before drying on the blot. The blots containing the dried samples were blocked with 5% skim milk in Tris-buffered saline Tween-20 (TBST; 10 mM Tris–HCl, pH 7.4, 0.15 M NaCl, 0.1% Tween-20) for 1 h. After blocking, the blots were rinsed twice in TBST and incubated in the absence of primary antibody (−Ab) as a negative control or with either the anti-NLS1 antibody (+anti-NLS1) or the anti-NLS2 antibody (+anti-NLS2), each at a concentration of 1 μg/ml, in TBST containing 1% bovine serum albumin (BSA) for 1 h. The blots were then rinsed twice with TBST for 1 min each and labeled with horseradish peroxidase conjugated to goat anti-rabbit secondary (Sigma, St. Louis, MO) in TBST containing 1% BSA for 1 h. After secondary antibody incubation, the blots were rinsed again twice with TBST for 1 min each and then washed twice for 30 min each in TBS containing 1% Triton X-100. The blots were developed with ECL (GE Healthcare) for visualization. In each case, "/5" denotes a sample applied at a concentration fivefold more dilute than the corresponding sample on the left.

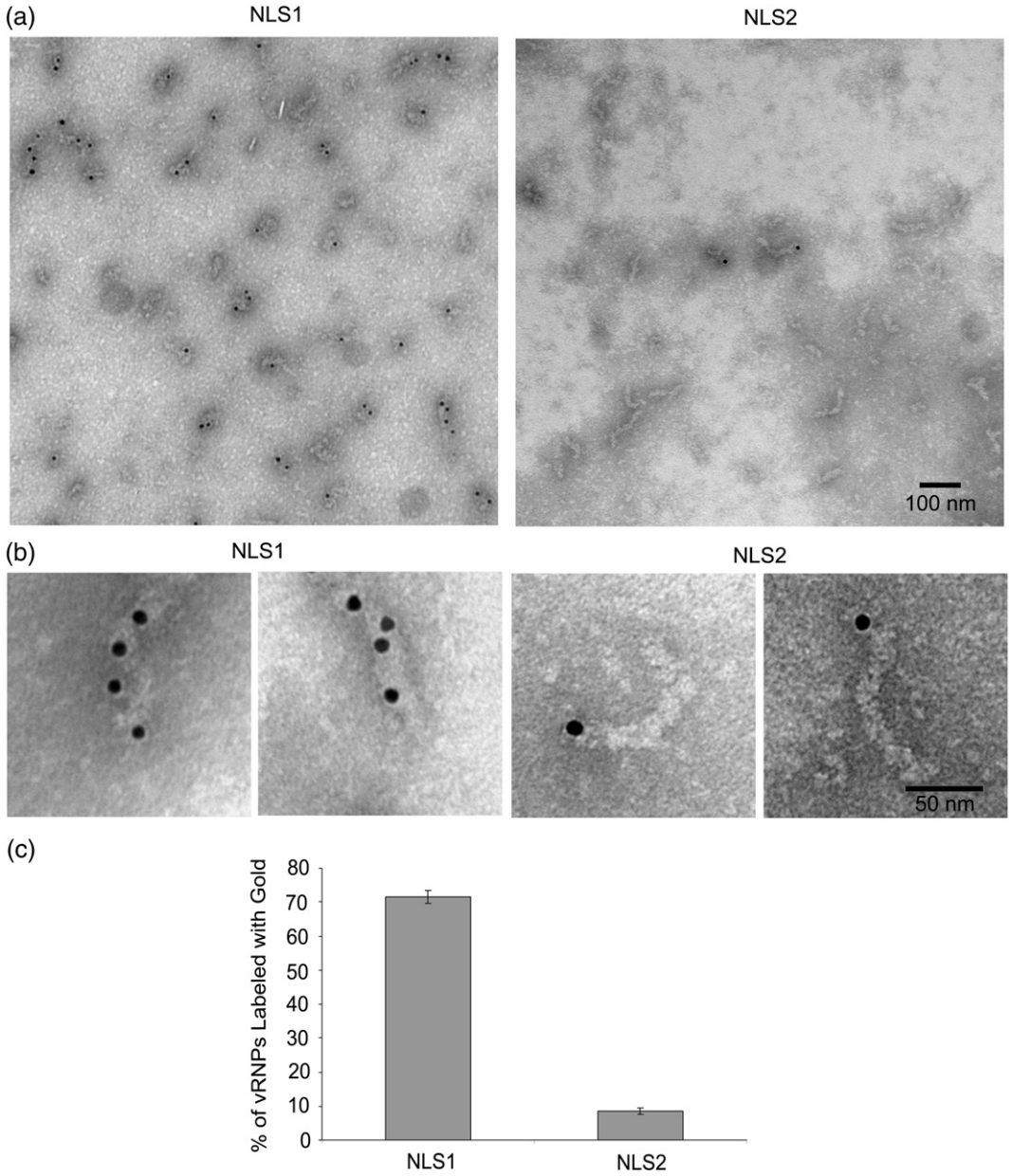

Fig. 2. (a and b) Immunogold electron microscopy of influenza vRNP labeled with the anti-NLS1 (left) or the anti-NLS2 (right) antibody. vRNPs were absorbed onto electron microscopy grids as described in Fig. 1b, and all steps were performed placing the grids in a wet chamber. Grids with absorbed vRNPs were blocked with 2% BSA in PBS (twice, for 5 min each) and incubated with primary antibody (anti-NLS1 or anti-NLS2, each at a concentration of 1 μg/ml) for 1 h. The grids were then washed with 0.2% BSA in PBS (four times, 5 min each) and incubated with gold-conjugated goat anti-rabbit secondary antibody (Ted Pella) for 1 h. This was followed by four washes in PBS containing 0.2% BSA (5 min each) and another three washes in PBS (5 min each). The samples were fixed with 1% glutaraldehyde in PBS for 5 min, washed with distilled water, and then negatively stained with 1% ammonium molybdate before viewing under a Hitachi H7600 TEM. (c) Quantitative analysis of the number of vRNPs that were labeled with the antibodies for the experiments described above. For each condition, 500 vRNP particles were scored.

each vRNP than did the anti-NLS2 antibody. Quantitative analysis of the gold particles showed that 71% of the vRNP molecules had gold particles associated with them when the anti-NLS1 antibody was used, while less than 10% of the vRNPs had gold particles associated when the anti-NLS2 antibody was used (Fig. 2c). Moreover, while gold labeling was found throughout the vRNP molecule for the anti-NLS1 antibody, labeling often occurred at one end of the vRNP for the anti-NLS2 antibody (Fig. 2b). In agreement with the dot-blot experiments, these electron microscopy results therefore suggest that NLS2 may be hidden by oligomeric interactions either from the assembly of NP molecules or from its interaction with the vRNA. NLS1, on the other hand, is so close to the N terminus of NP that it is more readily exposed and can thus bind to its target more readily. Taken together, these

results of immunogold labeling of vRNPs show that NLS1 is more exposed on the intact vRNP molecule than NLS2, supporting previous results that NLS1 is the main NLS that mediates the nuclear import of influenza vRNPs.[12]

To better understand the arrangement of NP oligomers within each vRNP molecule, we analyzed in more detail the binding of the anti-NLS1 antibody to vRNPs. It is well established that in the vRNP structure, the NP oligomeric arrangement is assembled as a ribbonlike cord annealed at its ends and coils to form a double-helical structure with a loop at one end (Fig. 4c).[4,21–23] To determine the periodicity of repeat of NP molecules within the helical structure, we chose vRNPs immunogold labeled with the anti-NLS1 antibody that have two or more associated gold particles positioned to one side of the vRNP (Fig. 3a) and determined the minimum separation of the gold particles in these vRNPs. As shown on the histogram in Fig. 3b, the minimum distance between gold particles was approximately 22 nm. Thus, the NLS1 epitopes recognized by the antibody on one side of the vRNPs are approximately 22 nm apart. It is possible that the periodicity of repeat could be 11 nm, instead of 22 nm, since the gold-labeled secondary antibody could find it sterically hindered to bind to an existing anti-NLS1 antibody that was too close in proximity. A minimum separation of 22 nm between NLS1 epitopes on one side of the vRNP would be in agreement with approximately four layers of NP monomers stacked on top of each other in the structure of the vRNP (Fig. 4c). This is because a single monomer is approximately 5.5 nm in height, as we measured from the crystal structure of NP[9] using Deepview.[24] Thus, the periodicity of repeat of NP molecules within the double-helical structure of vRNP would be twice of 5.5 nm, or 11 nm (Fig. 4c).

Taking into account the data from Fig. 3 and previous structural data on vRNP complexes,[4,6,9,18–20] we present a model on the structure and assembly of vRNPs derived from influenza A (Fig. 4). Normally, if only NP molecules are present in the absence of any vRNA, NP monomers exist in equilibrium with NP in its closed-structure, oligomeric form, commonly found as trimers.[9] However, helical structures of assembled NP can also be present in the absence of any RNA.[20] These closed oligomeric structures of NP form likely because of the natural affinity of NP to bind to adjacent NP molecules. In addition, having the presence of short single-stranded RNA segments also allows NP to form these small oligomers.[9] However, if longer segments of RNA are present (>400 nt[6]), as in the case of vRNP complexes derived from influenza virions, the NP oligomeric ring twists to form a double-helical conformation with a highly regular periodicity of repeat (Fig. 4c). Our analysis indicates that the repeat of the helix is 11 nm and that the multiple copies of NLS1 are highly exposed throughout the vRNP molecule. This is likely because NLS1 is located at the N-terminal tip of NP, which is not involved in the oligomerization of NP. NLS2, on the other hand, may be hidden by interactions with the vRNA or adjacent NP subunits and would be more rarely exposed. When NLS2 is exposed (Fig. 2), it is usually located at one end of the molecule, perhaps because the vRNA is interacting with its viral polymerases at that end of the vRNP instead of interacting with NP molecules.

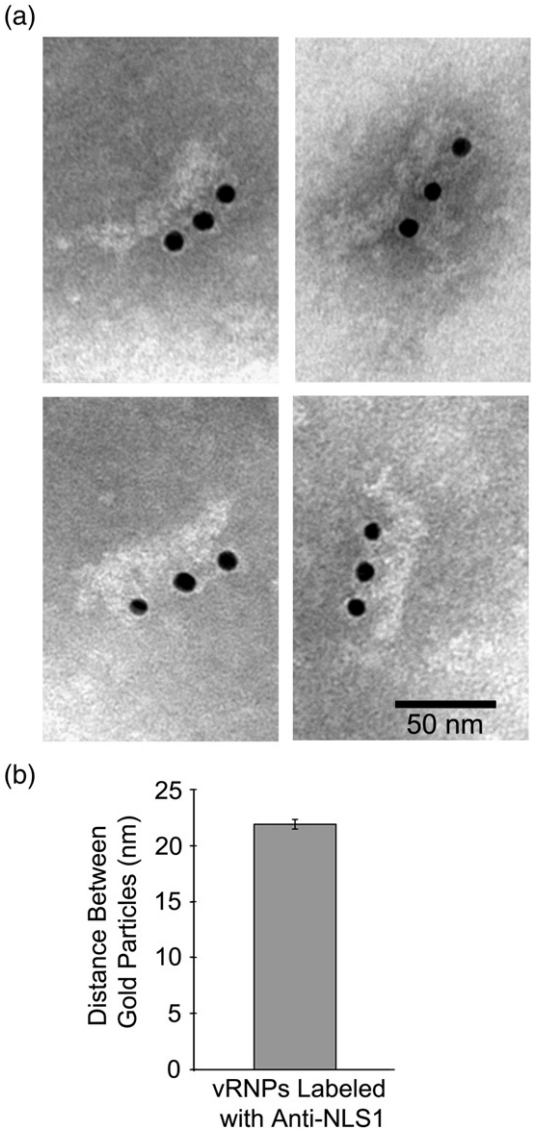

Fig. 3. Quantitative analysis of the periodicity of immunogold particles associated with vRNPs labeled with the anti-NLS1 antibody. (a) Representative vRNP samples used for quantitation. vRNPs containing gold particles positioned on one side of a vRNP imaged in as straight a conformation as possible were chosen for the quantitation. (b) Graphical analysis of the minimum distance between the gold particles. The software Carnoy (Laboratory of Plant Systematics, Leuven, Belgium) was used to measure the distances between gold particles. Fifty distances were scored.

Better understanding the arrangement and assembly of NP and the RNA within vRNP complexes is critical to effectively disrupting potential binding sites on the complex. For example, better understanding

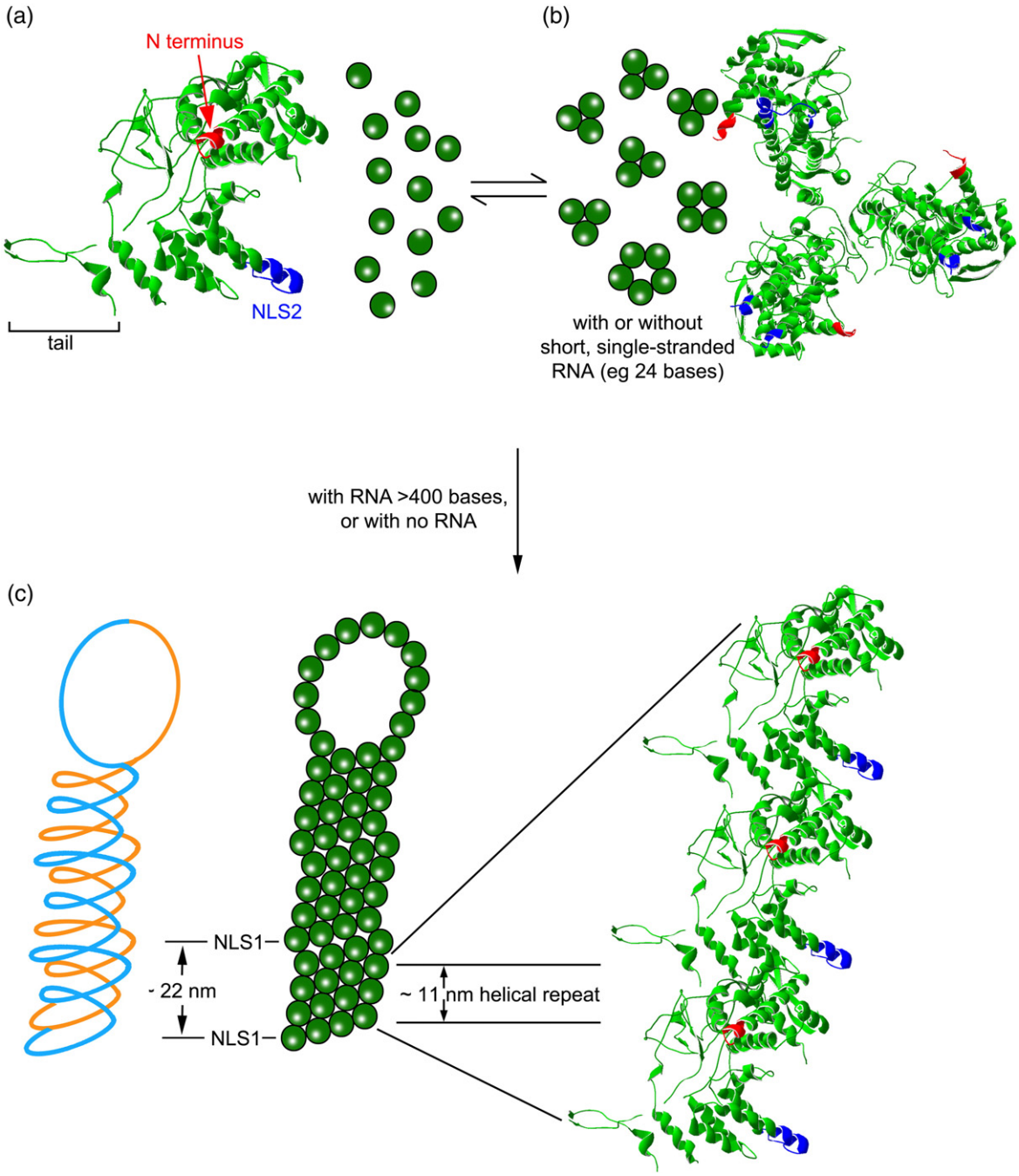

Fig. 4. Models of influenza NP and vRNP. The vRNP models were constructed from data in this study and several publications from other labs.[4,6,9,18–20] (a) Ribbon model of the monomeric NP crystal structure, with the first six residues of the N terminus (^{21}NATEIR^{26}) present in the crystal structure shown in red and the residues in NLS2 (^{198}KRGINDRNFWRGENGRKTR^{216}) present in the crystal structure in blue. The tail region is involved in intermolecular interactions with adjacent NP subunits in oligomeric NP. (b) Closed structures of oligomeric NP. In the absence of RNA or in the presence of short single-stranded RNA of approximately 24 bases, NP forms closed structures, mainly trimers, as well as larger oligomers. (c) Helical oligomeric NP. NP forms a helical structure in vRNPs in the presence of RNA longer than 400 bases or in the absence of any RNA. The model on the left depicts the double-helical coil of oligomeric NP, with the area in light blue comprising one-half of the NP oligomeric strand and that in orange comprising the other half of a contiguous NP oligomeric strand. The model in the middle shows the front face of the helical arrangement of NP, with each green circle representing one molecule of NP. The model on the right shows the crystal structure of three NP molecules stacked on top of each other within the structure of the vRNP. Each NP monomer is approximately 5.5 nm in height, giving a helical repeat of 11 nm. This value corresponds to half of the distance between NLS1 epitopes found on the vRNP (Fig. 3).

the location and number of sites of exposure of the key NLSs on influenza vRNPs will allow for more effective disruption of its nuclear localization function. Since we found in the present study that both NLS1 and NLS2 are exposed in intact vRNPs purified from influenza virions, disrupting both NLSs is therefore critical to disrupting its nuclear import, supporting previous findings.[12] Since we also quantified that 71% of vRNPs contain an exposed NLS1, usually with one to three (and sometimes up to six) gold particles bound per vRNP, and that less than 10% of vRNPs contain an exposed NLS2, these quantitations provide an idea about the approximate levels of inhibition required to abolish the nuclear import capabilities of vRNPs. In addition, the highly regular periodicity of repeat in the structure of vRNPs, as indicated by the regular distances found between gold particles, appears to be critical. Therefore, bioactive compounds that interfere with the formation of such regular repeats in the vRNP structure may also disrupt its function in nuclear import, the transcription of new influenza viral genes, or the nuclear export of newly synthesized and assembled vRNPs from host cells.

Acknowledgements

This work was supported by grants from the Canadian Institute of Health Research and the Natural Sciences and Engineering Research Council of Canada.

References

1. Lamb, R. A. & Krug, R. M. (2001). Orthomyxoviridae: the virus and their replication. In *Fields Virology* (Knipe, D. M. & Howley, P. M., eds), pp. 1487–1532, Lippincott Williams & Wilkins, Philadelphia, PA, USA.
2. Noda, T., Sagara, H., Yen, A., Takada, A., Kida, H., Cheng, R. H. & Kawaoka, Y. (2006). Architecture of ribonucleoprotein complexes in influenza A virus particles. *Nature*, **439**, 490–492.
3. Harris, A., Cardone, G., Winkler, D. C., Heymann, J. B., Brecher, M., White, J. M. & Steven, A. C. (2006). Influenza virus pleiomorphy characterized by cryoelectron tomography. *Proc. Natl Acad. Sci. USA*, **103**, 19123–19127.
4. Compans, R. W., Content, J. & Duesberg, P. H. (1972). Structure of the ribonucleoprotein of influenza virus. *J. Virol.* **10**, 795–800.
5. Baudin, F., Bach, C., Cusack, S. & Ruigrok, R. W. (1994). Structure of influenza virus RNP: I. Influenza virus nucleoprotein melts secondary structure in panhandle RNA and exposes the bases to the solvent. *EMBO J.* **13**, 3158–3165.
6. Ortega, J., Martin-Benito, J., Zurcher, T., Valpuesta, J. M., Carrascosa, J. L. & Ortin, J. (2000). Ultrastructural and functional analyses of recombinant influenza virus ribonucleoproteins suggest dimerization of nucleoprotein during virus amplification. *J. Virol.* **74**, 156–163.
7. Prokudina-Kantorovich, E. N. & Semenova, N. P. (1996). Intracellular oligomerization of influenza virus nucleoprotein. *Virology*, **223**, 51–56.
8. Elton, D., Medcalf, E., Bishop, K. & Digard, P. (1999). Oligomerization of the influenza virus nucleoprotein: identification of positive and negative sequence elements. *Virology*, **260**, 190–200.
9. Ye, Q., Krug, R. M. & Tao, Y. J. (2006). The mechanism by which influenza A virus nucleoprotein forms oligomers and binds RNA. *Nature*, **444**, 1078–1082.
10. Luo, M., Green, T. J., Zhang, X., Tsao, J. & Qiu, S. (2007). Structural comparisons of the nucleoprotein from three negative strand RNA virus families. *Virol. J.* **4**, 72.
11. Kemler, I., Whittaker, G. & Helenius, A. (1994). Nuclear import of microinjected influenza virus ribonucleoproteins. *Virology*, **202**, 1028–1033.
12. Wu, W. W. H., Sun, Y. H. B. & Pante, N. (2007). Nuclear import of influenza A viral ribonucleoprotein complexes is mediated by two nuclear localization sequences on viral nucleoprotein. *Virol. J.* **4**, 49.
13. Neumann, G., Castrucci, M. R. & Kawaoka, Y. (1997). Nuclear import and export of influenza virus nucleoprotein. *J. Virol.* **71**, 9690–9700.
14. Weber, F., Kochs, G., Gruber, S. & Haller, O. (1998). A classical bipartite nuclear localization signal on Thogoto and influenza A virus nucleoproteins. *Virology*, **250**, 9–18.
15. Wang, P., Palese, P. & O'Neill, R. E. (1997). The NPI-1/NPI-3 (karyopherin alpha) binding site on the influenza A virus nucleoprotein NP is a nonconventional nuclear localization signal. *J. Virol.* **71**, 1850–1856.
16. Cros, J. F., Garcia-Sastre, A. & Palese, P. (2005). An unconventional NLS is critical for the nuclear import of the influenza A virus nucleoprotein and ribonucleoprotein. *Traffic*, **6**, 205–213.
17. Ozawa, M., Fujii, K., Muramoto, Y., Yamada, S., Yamayoshi, S., Takada, A. *et al.* (2007). Contributions of two nuclear localization signals of influenza A virus nucleoprotein to viral replication. *J. Virol.* **81**, 30–41.
18. Martin-Benito, J., Area, E., Ortega, J., Llorca, O., Valpuesta, J. M., Carrascosa, J. L. & Ortin, J. (2001). Three-dimensional reconstruction of a recombinant influenza virus ribonucleoprotein particle. *EMBO Rep.* **2**, 313–317.
19. Klumpp, K., Ruigrok, R. W. & Baudin, F. (1997). Roles of the influenza virus polymerase and nucleoprotein in forming a functional RNP structure. *EMBO J.* **16**, 1248–1257.
20. Ruigrok, R. W. & Baudin, F. (1995). Structure of influenza virus ribonucleoprotein particles: II. Purified RNA-free influenza virus ribonucleoprotein forms structures that are indistinguishable from the intact influenza virus ribonucleoprotein particles. *J. Gen. Virol.* **76**, 1009–1014.
21. Heggeness, M. H., Smith, P. R., Ulmanen, I., Krug, R. M. & Choppin, P. W. (1982). Studies on the helical nucleocapsid of influenza virus. *Virology*, **118**, 466–470.
22. Jennings, P. A., Finch, J. T., Winter, G. & Robertson, J. S. (1983). Does the higher order structure of the influenza virus ribonucleoprotein guide sequence rearrangements in influenza viral RNA? *Cell*, **34**, 619–627.
23. Pons, M. W., Schulze, I. T., Hirst, G. K. & Hauser, R. (1969). Isolation and characterization of the ribonucleoprotein of influenza virus. *Virology*, **39**, 250–259.
24. Schwede, T., Kopp, J., Guex, N. & Peitsch, M. C. (2003). SWISS-MODEL: an automated protein homology-modeling server. *Nucleic Acids Res.* **31**, 3381–3385.